Downloaded from orbit.dtu.dk on: Dec 20, 2017

Technical University of Denmark

Smartphones as pocketable labs: Visions for mobile brain imaging and neurofeedback

Stopczynski, Arkadiusz; Stahlhut, Carsten; Petersen, Michael Kai; Larsen, Jakob Eg; Jensen, Camilla Birgitte Falk; Ivanova, Marieta Georgieva; Andersen, Tobias; Hansen, Lars Kai

Published in:
International Journal of Psychophysiology

Link to article, DOI:
10.1016/j.ijpsycho.2013.08.007

Publication date:
2014

Document Version
Early version, also known as pre-print

Link back to DTU Orbit

Citation (APA):
Stopczynski, A., Stahlhut, C., Petersen, M. K., Larsen, J. E., Jensen, C. B. F., Ivanova, M. G., ... Hansen, L. K. (2014). Smartphones as pocketable labs: Visions for mobile brain imaging and neurofeedback. International Journal of Psychophysiology, 91(1), 54–66. DOI: 10.1016/j.ijpsycho.2013.08.007

DTU Library
Technical Information Center of Denmark

General rights
Copyright and moral rights for the publications made accessible in the public portal are retained by the authors and/or other copyright owners and it is a condition of accessing publications that users recognise and abide by the legal requirements associated with these rights.

- Users may download and print one copy of any publication from the public portal for the purpose of private study or research.
- You may not further distribute the material or use it for any profit-making activity or commercial gain
- You may freely distribute the URL identifying the publication in the public portal

If you believe that this document breaches copyright please contact us providing details, and we will remove access to the work immediately and investigate your claim.

Smartphones as Pocketable Labs: Visions for Mobile Brain Imaging and Neurofeedback

Arkadiusz Stopczynski[1,*], Carsten Stahlhut, Michael Kai Petersen, Jakob Eg Larsen, Camilla Falk Jensen, Marieta Georgieva Ivanova, Tobias S. Andersen, Lars Kai Hansen

Technical University of Denmark, Department of Applied Mathematics and Computer Science, Section for Cognitive Systems, Building 303B. DK-2800 Kgs. Lyngby, Denmark.

Abstract

Mobile brain imaging solutions, such as the *Smartphone Brain Scanner*, which combines low cost wireless EEG sensors with open source software for real-time neuroimaging, may transform neuroscience experimental paradigms. Normally subject to the physical constraints in labs, neuroscience experimental paradigms can be transformed into dynamic environments allowing for the capturing of brain signals in everyday contexts. Using smartphones or tablets to access text or images may enable experimental design capable of tracing emotional responses when shopping or consuming media, incorporating sensorimotor responses reflecting our actions into brain machine interfaces, and facilitating neurofeedback training over extended periods. Even though the quality of consumer neuroheadsets is still lower than laboratory equipment and susceptible to environmental noise, we show that mobile neuroimaging solutions, like the *Smartphone Brain Scanner*, complemented by 3D reconstruction or source separation techniques may support a range of neuroimaging applications and thus become a valuable addition to high-end neuroimaging solutions.

Keywords: Mobile sensor, real-time, EEG, neuroimaging, source reconstruction, brain monitoring, brain-computer interface.

1. Introduction

Only recently have wireless neuroheadsets, capable of capturing changing electrical potentials from brain activity through electrodes placed on the scalp

*Corresponding author

Email addresses: arks@dtu.dk (Arkadiusz Stopczynski), csta@dtu.dk (Carsten Stahlhut), mkai@dtu.dk (Michael Kai Petersen), jaeg@dtu.dk (Jakob Eg Larsen), cbfj@dtu.dk (Camilla Falk Jensen), mgiv@dtu.dk (Marieta Georgieva Ivanova), toban@dtu.dk (Tobias S. Andersen), lkai@dtu.dk (Lars Kai Hansen)

[1] *Phone number:* +45 45253899

using Electroencepahlography (EEG), made mobile brain imaging a reality. The emergence of low-cost EEG sensors and the increasing computational power of smartphones may transform neuroimaging from constrained laboratory settings to experimental paradigms, allowing us to model mental state in an everyday context. This presents a paradigm shift, making it possible to design new types of experiments that characterize brain states during natural interaction over extended periods of time. Until recently most neuroimaging experiments have been performed with subjects who are at rest, under the assumption the brain responses being measured will not be influenced by subjects sitting or laying down. However, this may be inaccurate, as animal studies using mice indicate that neurons in the visual cortex double their visually evoked firing rates if they run on a treadmill rather than stand still [1]. Since the discovery of parietal-frontal circuits of mirror neurones, which fire both when we grasp an object and when we observe others doing the same [2] [3], the sensorimotor system can no longer be considered as only involved with motion. Consequently, these mechanisms should rather be understood as forming an integral part of cognition, allowing us to generalize the goals of actions based on motor representations in the brain [4].

While there is already significant literature concerned with dynamic brain states during natural complex stimuli in conventional laboratory experiments, see e.g., [5, 6, 7], there has been a growing call to design studies that relax the constraints of the lab and widen the focus to map out how we perceive our surroundings under naturalistic conditions [8]. For example, natural motion has been incorporated into laboratory experiments using tools such as the MoBI Lab Matlab plugin [9] in order to correlate motion capture data of moving limbs with the brain responses being triggered [10]. Even adding a few degrees of freedom may provide an understanding of how cortical responses differ by simply changing posture [11], either by measuring how theta brainwave activity is attenuated in sleepy subjects once they stand up [12], or by analyzing the modulation in spectral power within alpha and beta brainwaves appearing when one foot hits the ground and the other foot is lifted, as subjects are no longer transfixed on a chair in front of a computer screen [13]. This provides a foundation for extending standard EEG paradigms, such as the P300 event-related potential, to measure how we consciously perceive visual objects when participants are no longer required to sit motionless but are able walk on a belt during the experiment [14]. It also makes it possible to eventually move a P300 experiment outside the lab, as has recently been demonstrated by Debener and colleagues [15] by combining the wireless hardware from a consumer neuroheadset[2] with standard EEG cap electrodes [3] and using a laptop to record the cortical responses, thus providing a portable lab which can be stored in a backpack and easily carried by the subjects participating in the experiment.

Taking the idea of bringing EEG into the wild one step further, the *Smart-*

[2] emotiv.com

[3] easycap.de/easycap

Figure 1: SBS2 mobile EEG recording with real-time 3D source reconstruction, on an Android smartphone connected wirelessly to an Easycap 16 electrode setup based on Emotiv hardware.

phone Brain Scanner (SBS2) open-source software project (`http://github.com/SmartphoneBrainScanner`) introduced in [16, 17], makes it possible to build brain imaging applications for real-time 3D source reconstruction or neurofeedback training. By combining a wireless EEG cap with an Android smartphone or tablet, the SBS2 allows for presenting time-locked audiovisual stimuli such as text, images, or video, and it allows for capturing elicited neuroimaging responses on the mobile device, thereby transforming low-cost consumer hardware into a pocketable brain imaging lab. As the *Smartphone Brain Scanner* project potentially allows for designing novel types of brain imaging paradigms, we have initially validated the SBS2 framework in three experiments related to BCI motor control, embodied semantics, and neurofeeedback interfaces in order to illustrate the feasibility of capturing mental state in a mobile context. In the following sections we briefly review existing mobile EEG sensors, outline the architectural design of the *Smartphone Brain Scanner* system for real-time 3D reconstruction, describe aspects of source separation and spatial filtering in relation to mobile brain imaging, and give examples of applications built on top of the open-source software framework for mobile Android devices related to imagined finger tapping, emotional responses to text, and design of neurofeedback interfaces.

2. Mobile EEG acquisition

A wide range of prototype electrode designs, suitable for mobile neuroimaging, are currently under development, based on MEMS microelectromechanical systems utilizing spring-loaded dry contact pins or hard carbon nanotubes that press against the scalp [18]. For long-term EEG measurement without gel, another option is electrodes made from soft foam covered with conductive fabric [19], or new types of non-contact high input impedance sensors capable of capturing EEG signals on the basis of capacitive coupling [20], even when resting on top of several layers of hair. In contrast to gel-based EEG electrodes, dry contacts need no skin preparation, and can therefore more easily be utilized for neuroimaging as participants are able to put on a neuroheadset without any assistance. However, even though pin or nanotube contacts easily penetrate the hair and therefore offer more possibilities for placement than conductive foam-based sensors attached to the skin of the forehead, a spring-like setup may still be susceptible to noise when users move. Capacitive sensors provide an alternative for unobtrusive physiological monitoring, but require an integrated ultra-high impedance frontend for non-contact biopotential sensing [21]. So-called Ear-EEG is a promising technology for long-term EEG data collection, offering improved comfort and aesthetics [22]. Benchmarks of prototype capacitive non-contact and mechanical sensors in an experiment related to decoding a steady state visual evoked potential in the 8-13 Hz frequency band showed only little signal degradation when compared to standard gel-based Ag/AgCl electrodes [20], showing that these novel sensors may, in longer term, provide the increased usability that may assure the transformation of neuroimaging from fixed laboratory setups to an everyday mobile context.

Among existing commercial solutions, the ThinkGear module manufactured by NeuroSky[4] provides the foundation for several EEG consumer products which integrate a single dry electrode along with a reference and a ground attached to a headband. It provides A/D conversion and amplification of one EEG channel, is capable of capturing brain wave patterns in the 3-100 Hz frequency range, and records at $512Hz$ sampling rate. Even a single-channel EEG setup, using a passive dry electrode, such as the NeuroSky, positioned at the forehead and a reference (typically an earlobe), may allow for measuring mental concentration and drowsiness by assessing the relative distribution of brainwave frequencies [23]. More comfortable neuroheadsets using conductive Ni/Cu covered polymer foam, such as Mindo[5], measure brain activity from the forehead on three EEG electrodes plus a reference channel attached to the earlobe. Integrating analog to digital conversion at 256 Hz sampling rate for acquisition of bandpass filtered signals in the 0.5-50 Hz range, the neuroheadset offers 23 hours of battery life and wireless Bluetooth communication, and has been demonstrated in BCI brain machine interfaces used in games based on controlling the

[4] http://www.neurosky.com/Products/ThinkGearAM.aspx
[5] http://www.mindo.com.tw/en/index.php

power of alpha brainwave activity [24]. Other consumer neuroheadsets such as the Emotiv EEG[6], provide both wireless communication via a USB dongle and analog to digital conversion of 16 EEG channels (including reference and ground) at $128Hz$ sampling rate while using moist felt-tipped sensors which press against the scalp with a simple spring-like design. Originally designed as a mental game controller capable of tracing emotional responses and facial expressions, the majority of electrodes are placed over the frontal cortex and have no midline positions (AF3, F7, F3, FC5, T7, P7, O1, O2, P8, T8, FC6, F4, F8, AF4 with P3/P4 used as reference and ground). However, as mentioned earlier, Debener and colleagues [15] recently demonstrated that it is possible to merge the wireless hardware from the Emotiv neuroheadset with high quality, conductive, gel-based electrodes in a standard EEG cap[7]. Repackaging the electronics and battery into a small box ($49mm \times 44mm \times 25mm$) which can be attached to the EEG cap and rewired through a connector plug to 16 sintered Ag/AgCl ring electrodes can occur, thus providing a fully customizable montage which allows the electrodes to be freely placed in the EEG cap according to the 10-20 international system (in the present experiment Fpz, F3, Fz, F4, C3, Cz, C4, TP9, TP10, P3, Pz, P4, O1, O2 with AFz/FCz used as reference and ground).

We have tested both the original Emotiv neuroheadset as well as the modified EEG cap setup in connection with the *Smartphone Brain Scanner* open-source software project in the experimental designs outlined below.

3. Software Framework: Smartphone Brain Scanner

The *Smartphone Brain Scanner* (SBS2) is a software platform for building research and end-user oriented multi-platform EEG applications. The focus of the framework is on mobile devices (smartphones, tablets) and on consumer-grade (low-density and low-cost) mobile neurosystems. SBS2 is freely available under an MIT License at `https://github.com/SmartphoneBrainScanner`. Additional technical details about the framework can be found in [25].

The framework is divided into three layers: low-level data acquisition, data processing, and applications. The first two layers constitute the core of the system and include common elements used by various applications. The architecture is outlined in Figure 2.

3.1. Key Features

With focus on the mobile devices, SBS2 is a multi-platform framework. The underlying technology – Qt – is an extension of C++ programming language and is currently supported on the main desktop operating systems (Linux, OSX, Windows) as well as mobile devices (Android, BB10, partially iOS) (see `http://qt.digia.com/Product/Supported-Platforms/`).

[6] http://www.emotiv.com
[7] http://easycap.de/easycap

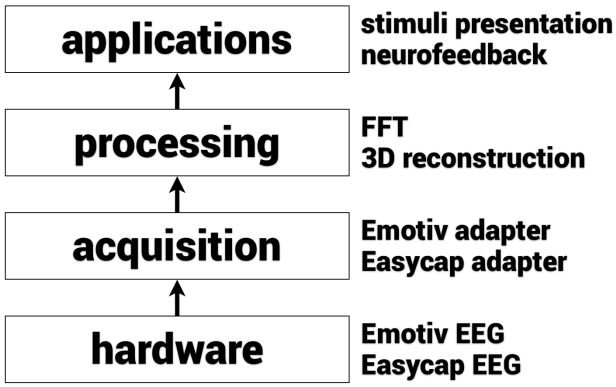

Figure 2: Layered architecture of the SBS2 framework. Data from connected EEG hardware is extracted by specific adapters, processed, and used by the applications.

The additional acquisition and processing modules can be created as C++ classes and integrated directly with the core of the framework. The framework supports building real-time applications; data can be recorded for subsequent offline analysis, most of the implemented data processing blocks aim to provide real-time functionality for working with the EEG signal. The applications developed with SBS2 are applications in the full sense, as they can be installed on desktop and mobile devices, can be started by the user in the usual way, and can be distributed via regular channels, such as repositories and application stores.

The most demanding data processing block is the real-time source reconstruction aimed at producing 3D images as demonstrated in Figure 4. Source reconstruction is carried out using Bayesian formulation of either the widely used Minimum-norm method (MN) [26] or the low resolution electromagnetic tomography (LORETA) [27]. Further description about the inverse methods implemented in the *Smartphone Brain Scanner* will be given later.

4. Methods

4.1. Brain Computer Interface Based on Imagined Finger Tapping

One of the arguably most widely used paradigms of the brain computer interface literature is a task in which a subject is instructed to select between two or more different imagined movements [28, 29, 30, 31]. Mental imagery is the basis of many BCI systems, originally conceived to assist patients with severe disabilities to communicate by 'thought'. The rationale is that the patient, while having problems carrying out the actual movements, may still be able to plan the movement and thereby produce a stable motor-related brain activity, which can

Figure 3: SBS2 mobile neuroimaging apps for neurofeedback training, presentation of experimental stimuli, and real-time 3D source reconstruction, running on Android mobile devices via a wireless connection to an Emotiv or Easycap EEG setup.

be used as an input to the computer/machine. In this contribution we replicate a classical experiment with imagined finger tapping (left vs. right) inspired by [31]. The setup consisted of a set of three different images with instructions, *Relax*, *Left*, and *Right*. In order to minimize the effect of eye movements, the subject was instructed to focus on the center of the screen, where the instructions also appeared (3.5" display size, 800 x 480 pixels resolution, at a distance of 0.5 m).

The instructions *Left* and *Right* appeared in random order with an equal probability. A total of 200 trials were conducted for a single subject. We selected 3.5 sec duration for the 'active' instruction (*Left* or *Right*) and 1.75-2.25 sec randomly selected for the *Relax* task, similar to [31]. The main motivation for random duration of the *Relax* task was to minimize the effect of the subject anticipating and starting the task prior to the instruction. The experiment was conducted with an Emotiv EEG neuroheadset transmitting wirelessly to a Nokia N900 smartphone. To illustrate the potential for performing such a study in a completely mobile context, all stimulus delivery and data recording were carried out using the SBS2. Analysis and post-processing and decoding were conducted off-line using standard analysis tools. In particular, we applied a common spatial pattern (CSP) approach [28] to extract spatial filters which would maximize the variance for one class, while minimizing the variance of the other class and vice versa. A quadratic Bayesian classifier for decoding was applied on features transformed as in [28].

4.2. Source Reconstruction and Source Separation

Compared to standard EEG laboratory setups, mobile neuroimaging is extremely susceptible to noise, as the ability to move around simultaneously introduces artifacts into the neuroimaging data induced by the EEG sensors, as well as originating from motion-related muscle activity. Likewise, mobile neuroimaging is much more exposed to environmental noise than experiments taking place under controlled conditions in a shielded laboratory. Combining sensor and source features, however, has been shown to improve classification in brain computer interaction BCI [32], even though these paradigms often involve activation of sensorimotor circuits where the location of sources is already quite well known. There might be an even larger potential by integrating source information for decoding complex brain states involving a range of different cognitive tasks. In particular, spectral analysis of changes in power may offer additional information on activity within specific brainwave bands, which, based on the frequency, determines whether it reflects local or more distributed cortical field potentials. We therefore suggest that incorporating prior knowledge on what constitutes brain-generated signals may overall enhance the feasibility of performing experiments using mobile neuroimaging solutions, see also [33].

One approach to localize the actual brain activity in EEG is to tackle the inverse problem of retrieving the distribution of underlying sources from a scalp map by using a forward head model to estimate the projection weights which are captured by the electrodes. The problem is, however, severely ill-posed, as typically tens of EEG electrodes will capture volume conducted brain activities which may have been generated by tens of thousands of equivalent dipoles representing post-synaptic activity within macrocolumns of the cortex [26, 27, 34]. A regularization that reduces the number of solutions is therefore applied, using methods such as low resolution electromagnetic tomography (LORETA), which assumes both the activity of neighboring neurons is synchronized and their orientation and strength can be modeled as point sources in a 3D grid reflecting 'blurred-localized' images of maximal activity [27]. With $\mathbf{F} \in \Re^{N_c \times N_v}$ representing the forward model relating the N_v cortical current sources, $\mathbf{V} \in \Re^{N_v \times N_t}$, to the N_c measured scalp electrodes, $\mathbf{X} \in \Re^{N_c \times N_t}$, the forward problem for a set of time points (N_t) is given by, $\mathbf{X} = \mathbf{FV} + \mathbf{E}$, when the noise contribution $\mathbf{E}$ is assumed additive. The Minimum-norm method (MN) [26] and LORETA methods can be represented as a single method, with MN as a special case of LORETA, namely, when no spatial coherence of neighboring sources is assumed as prior. From a Bayesian perspective the LORETA method is formulated as

$$p(\mathbf{X}|\mathbf{V}) = \prod_{t=1}^{N_t} \mathcal{N}\left(\mathbf{x}_t \left| \mathbf{F}\mathbf{v}_t, \beta^{-1}\mathbf{I}_{N_c}\right.\right) \quad (1)$$

$$p(\mathbf{V}) = \prod_{t=1}^{N_t} \mathcal{N}\left(\mathbf{v}_t \left| \mathbf{0}, \alpha^{-1}\mathbf{L}^T\mathbf{L}\right.\right) \quad (2)$$

in which β denotes the precision of the noise (inverse variance), α the precision parameter of the sources, and $\mathbf{L}$ the spatial coherence between the sources $\mathbf{V}$.

As the MN method assumes no spatial coherence between neighboring sources, the spatial coherence matrix becomes an identity matrix, $\mathbf{L} = \mathbf{I}$. In contrast, for LORETA this spatial coherence matrix typically takes the form of a graph Laplacian, implementing geometrical neighborhood driven smoothness. Given the likelihood,$p(\mathbf{X}|\mathbf{V})$, and prior distribution, $p(\mathbf{V})$, of the current sources, the most likely source distribution can be obtained by maximizing the posterior distribution over the sources as

$$\begin{aligned} p(\mathbf{V}|\mathbf{X}) &= \prod_{t=1}^{N_t} \mathcal{N}(\mathbf{v}_t|\boldsymbol{\mu}_t, \boldsymbol{\Sigma}_v) \\ \boldsymbol{\Sigma}_v &= \alpha^{-1}\mathbf{I}_{N_v} - \alpha^{-1}\mathbf{F}^T\boldsymbol{\Sigma}_x\mathbf{F}\alpha^{-1} \\ \boldsymbol{\Sigma}_x^{-1} &= \alpha^{-1}\mathbf{F}\mathbf{L}^T\mathbf{L}\mathbf{F}^T + \beta^{-1}\mathbf{I}_{N_c} \quad (3) \\ \bar{\mathbf{v}}_t &= \alpha^{-1}\mathbf{F}^T\boldsymbol{\Sigma}_x\mathbf{x}_t. \quad (4) \end{aligned}$$

The hyper-parameters α and β are optimized on-line using a standard Expectation-Maximization (EM) approach [35].

Rather than aiming to solve the inverse problem of determining the 'what' from 'where' of brain activity, an alternative approach is to apply methods based on higher-order statistics such as independent component analysis (ICA) [36]. This allows to separate individual processes ('what') when they stand out as temporally independent in the native, spatially overlapping scalp representation [37].

The ability of ICA to identify temporally independent events also allows for enhanced detection and automatic removal of artifacts [38]. Eye blinks manifest themselves as low $1-3Hz$ as well as higher frequency activity, which translates into stereotypical ICA scalp maps consisting of a single frontal dipole [39]. When comparing this method against a regression approach using an electrooculogram (EOG) eye movement correction procedure (EMCP) to remove eye blink artifacts, ICA turns out to yield almost perfect correction [40]. Also, other kinds of muscle activity stand out distinctly in the corresponding scalp maps. Overall, applying ICA as a preprocessing step improves artifact detection compared to analysis based on the raw EEG data [39]. With particular relevance to mobile neuroimaging, it has been demonstrated that independent component-based gait-artifact removal makes it possible to capture neural correlates in standard EEG experiments, even when walking or running [41].

EEG experiments have traditionally focused on analysis of event-related time-domain waveform deflections and frequency-domain perturbations in power, but neither of these approaches fully captures the underlying brain dynamics when averaging data over multiple trials, or ignoring phase resetting that contributes to the ERP [42]. When first applying ICA to the EEG data, the event-related time series waveforms come to represent independent components generated by temporally independent, physiologically decoupled local field potentials, and their corresponding scalp maps that resemble dipolar projections of the underlying sources [43]. This indicates that ICA may be used for more than denoising, e.g., it can be used to find the modes of event-related changes

in power, as the independent components framed by the dimensions of frequency, power, and phase consistency across trials. Even when electrodes are accurately placed, the recorded potentials may still vary due to individual differences in cortical surface and volume conduction. ICA may also here provide a common framework for comparison of the underlying brain activity in EEG data, regardless of the actual electrode positions. We thus compared ICA of the EEG data retrieved from both the Emotiv neuroheadset containing no central electrodes and the Easycap EEG montage including midline electrodes. In particular, we used the retrieved scalp maps and activation time series, as well as event-related changes in power spectra, to perform a statistical group comparison across experimental conditions and trials. As a preprocessing step, we reduced dimensionality based on principal component analysis (PCA) and subsequently applied K-means clustering to the independent components, in order to identify common patterns of brain activity across the two different mobile EEG setups [44].

4.3. Visual Stimulus to Investigate Emotional Responses

Over the past decades, neuroimaging studies have established that language is grounded in sensorimotor areas of the brain; highly related neuronal circuits seem involved whether we literally pick up a ball or in a phrase refer to grasping an idea [45]. Exploring whether such brain activation can be detected using a mobile EEG setup, the SBS2 framework was used to display the stimulus consisting of a subset of action verbs related to emotional expressions, face, and hand motion as used in a recent fMRI experiment [46]. The framework was also used to record the EEG signal for subsequent offline data analysis.

Two mobile 16 channel EEG setups were compared; the low cost Emotiv neuroheadset using saline sensors positioned laterally at AF3, F7, F3, FC5, T7, P7, O1, O2, P8, T8, FC6, F4, F8 and AF4 (P3/P4 used as Common Mode Sense (CMS) reference / Driven Right Leg (DRL) feedback) - versus a standard electrolyte gel-based EEG cap (Easycap, Germany) similar to what has previously been used for mobile P300 experiments [15] enabling an EEG setup including central and midline Ag/AcCl ring electrodes positioned at Fpz, F3, Fz, F4, C3, Cz, C4, TP9, TP10, P3, Pz, P4, O1 and O2 (AFz / FCz used as CMS reference / DRL feedback) according to the international 10-20 system.

A single subject pilot study was performed to compare the Emotiv and Easycap EEG setups based on 2×10 trials, each consisting of 3×20 action verbs presented in a randomized sequence on the smartphone display (Nokia N900). Each verb was exposed for $1000ms$ in a large white font on black background (3.5" display size, 800×480 pixels resolution) at a distance of $0.5m$, preceded by a fixation cross $500ms$ pre stimuli, and followed by $1000ms$ post stimuli black screen. Using the EEGLAB plug-in for MATLAB (MathWorks, USA), epoched EEG data was extracted offline (-500 ms to 1000 ms) and baseline corrected (-500 ms to 0 ms). As some of the recorded potentials are induced by muscle activity, we rejected abnormal data epochs by specifying that the spectrum should not deviate from baseline by +/- 50dB at 0-2Hz and manually removed

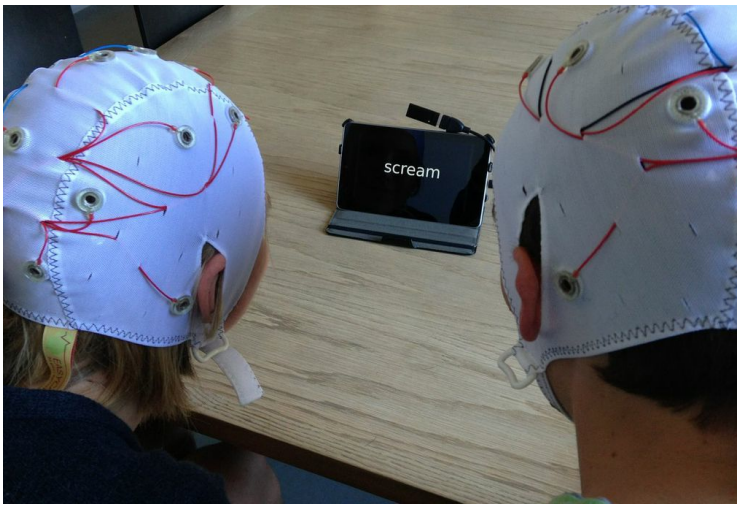

Figure 4: SBS2 app for presentation of visual stimuli and mobile EEG recording, using an Android tablet connected wirelessly to an Easycap 16 electrode setup based on Emotiv hardware.

eye blinks [44]. To facilitate a comparison between the different electrode placements used in the two experiments, we applied the extended Infomax algorithm to linearly project the EEG data recorded from individual electrodes onto a space of basis vectors, which were temporally independent from each other, using independent component analysis ICA to estimate the scalp maps and time courses of individual neural sources [39].

To assess the degree to which the Emotiv neuroheadset and the Easycap EEG setups capture common patterns in brain activity despite their differences in electrode montage, rather than simply measuring event-related responses from the 14 electrodes, we applied ICA in a single-subject study to retrieve 14 independent components from each of the 2×10 trials, related to the Emotiv and Easycap experiments, respectively: we analyzed $2 \times 10 \times 14$ independent components generated from the time-locked responses to reading 3×20 emotion, face, and hand-related action verbs in each trial. Retrieving the ICA components enabled us to initially compare the event related responses across the 3 action verb conditions, which in turn enabled us to identify similar independent sources within trials using the EEGLAB studyset functionality. Secondly, to identify common patterns of brain activity both within and across the Emotiv and Easycap experiments, the EEGLAB studyset functionality and MATLAB Statistical Toolbox were used to cluster the $2 \times 10 \times 14$, in total 280 ICs based on scalp maps, power spectra, and amplitude times series. After initially applying ICA for artifact rejection in each trial, the 280 ICA weights were recomputed as a basis for a statistical analysis using the EEGlab studyset functionality [44], where the dimensionality of the feature space was reduced to $N = 10$ by apply-

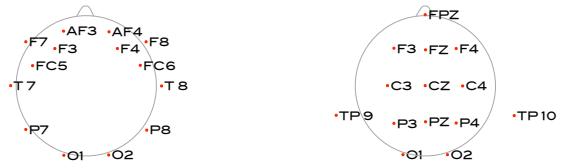

Figure 5: Electrode locations for two mobile 16 channel EEG setups; the Emotiv neuroheadset using saline sensors positioned laterally (left), versus a standard gel-based Easycap EEG montage including central and midline positions (right).

ing PCA principal component analysis [47]. The pre-clustering function PCA compresses the multivariate EEG features into a smaller number of mutually uncorrelated scalp projections, and computes a vector for each component to define normalized distances in a subspace representing the largest covariances in the ICA-weighted data. This means that the vectors contain the 10 highest PCA components for the ICA-weighted time series responses, scalp maps, and power, related to the three conditions. Next, the K-means algorithm ($K = 10$) was applied to cluster common ICA components within the 10 trials ($\sigma = 3$), related to the Emotiv neuroheadset (Figure 13) and the Easycap EEG setup (Figure 14), respectively. Comparing functionally equivalent groups of ICs makes it possible to assess whether they resemble recurring neural sources retrieved from multiple sessions, and to determine if the clustered ICs remain shared across the two different experimental EEG setups.

4.4. Mobile Interfaces for Neurofeedback

In contrast to personal informatics apps, neurofeedback interfaces require the user to interact in real time with audiovisual representations of EEG data in an attempt to control the ongoing brain activity. Neurofeedback experiments aiming to increase power in the upper alpha range have been shown to improve cognitive performance in several studies [48, 49]. While there is often a peak in individual alpha brainwave power around 10 Hz, neurofeedback training makes it possible to control and shift the activity towards the upper alpha range of 12 Hz. In relation to neurofeedback, an ability to consciously control alpha brainwave oscillations, which as a gating mechanism appears to be involved in selective attention [50], might thus potentially help explain the previously reported training effects on cognitive performance. Likewise, an association between higher alpha frequency and good memory performance has previously been shown [51].

However, designs for neurofeedback interfaces are often conceptualized with little attention to how the actual feedback of audiovisual elements might affect the user's ability to control brain activity. Normally, User Experience (UX) design of graphical interfaces involves initial modeling of user needs and selec-

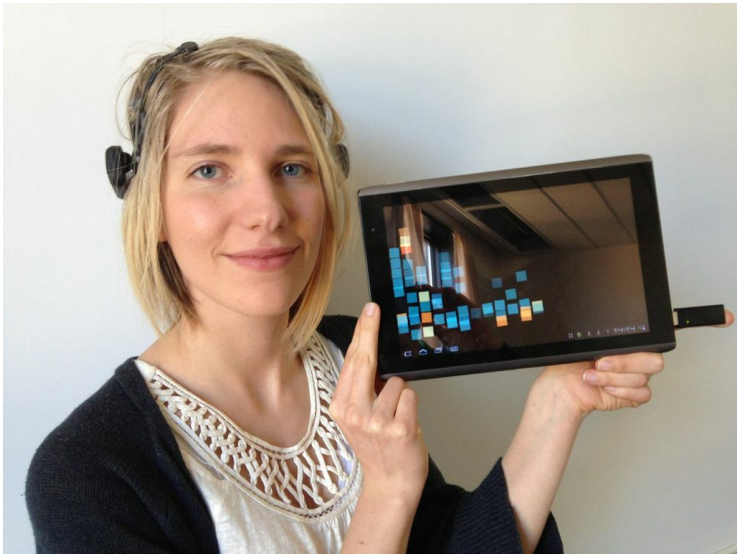

Figure 6: SBS2 neurofeedback training app running on an Android tablet, where a blue to orange shift in color horizontally over time represents an increase in upper alpha power.

tion of design patterns for organizing content and navigational layout reflecting gestalt principles. This may subsequently be translated into frameworks for interaction ranging from scrollable timeline lists to multilayered contextual map metaphors [52]. Neurofeedback applications on the other hand have typically concentrated on mapping EGG amplitude values directly onto audiovisual components. For example, sounds of ocean waves or high- or low-pitched gongs [53, 54] would map to visual designs based on vertical scales and squares of changing colors [55, 56, 49]. When targeted towards children, these elements have been incorporated into more complex scenarios built around airplanes, a 3D car racing environment, or a pole-vaulting cartoon mouse [57, 58]. In summary, these designs may be understood as based on contrasting combinations of the following audiovisual components [59]:

- pitch (low, high)
- volume (soft, loud)
- timbre (dark, light)
- duration (short, long)
- rhythm (temporal distribution)

- geometric primitives (connected segments)
- color (discrete, gradients)
- size (proximity, scalability)

- movement (horizontal, vertical)
- composition (spatial distribution)

To explore the influence such components might have on the efficacy of neurofeedback training, we tested two different interfaces developed for the SBS2. We conducted an experiment with 25 subjects aiming at increasing their upper alpha frequency band [60]. The neurofeedback experiment consisted of two iterations, testing the two different interfaces. In the first iteration, 12 healthy subjects (7 males and 5 females) with an average age of 23.6 ± 1.9 did neurofeedback training on a replication of an existing interface [49]. This interface indicated brain activity based on only two components (color gradients framed by a square primitive). In the second iteration another 13 healthy subjects (7 male and 6 female) with an average age of 26.6 ± 5.5 performed neurofeedback training using an interface developed on basis of the common features extracted from the first group of subjects. The second interface combined four components (scaled down color gradients framed by square primitives spatially distributed horizontally and vertically).

The EEG signal from all of Emotiv's 16 electrodes was recorded and the real-time feedback was constructed from O1 and O2. Additionally, an offline re-referencing of P3 and P4 with the frontal electrodes AF3, AF4, F3 and F4 allowed for P3 and P4 to be included in the later data processing, thus covering a larger area of the relevant cortical area. The power of the brain activity was calculated using Fast Fourier Transformation.

Both iterations consisted of five sessions during one week from Monday to Friday. Each session started and ended with a 5-minute baseline recording measuring the average brain activity during a simple task. In between the baseline recordings five 5-minute training sessions were conducted. After each session, we gathered qualitative data on the subjects thought patterns leading to an increase of alpha brain activity based on informal interviews. Each subject received a total of 25 training recordings and 10 baseline recordings.

The interface used in the first iteration was similar to the one used in a study by Zoefel et al. [49], where the feedback consisted of a square of changing colors gradually from blue, gray to red. Respectively each color represented real-time amplitudes below, equal to baseline, or above baseline, respectively, see Figure 7a. The subjects were instructed to make the square turn red. For the baseline recording a similar interface setup was used but with random color changes, making the visual stimuli similar to those of the training recordings and therefore more compatible. The subjects were asked to count the number of times the square turned red. This would ensure a similar cognitive task across the subjects while recording the baseline, thereby making these recordings comparable.

The feedback interface used in the second iteration consisted of small squares being generated once a second, if the alpha amplitudes exceeded the baseline. Over a 15 second interval the squares (maximum 15 squares) were assembled into a column, after which a new column of squares was incrementally generated

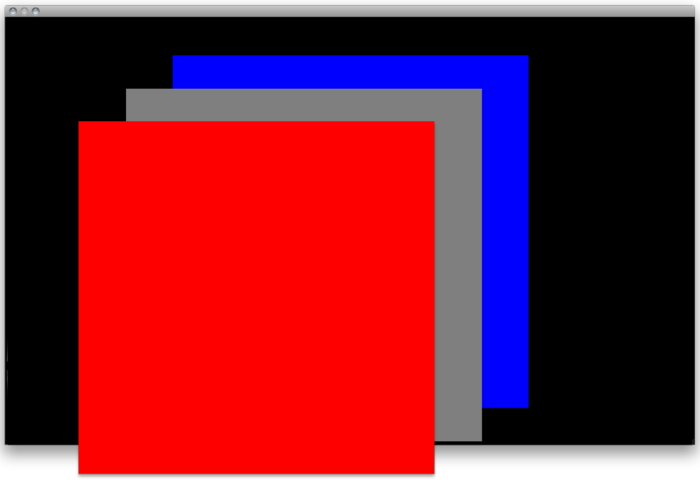

(a)

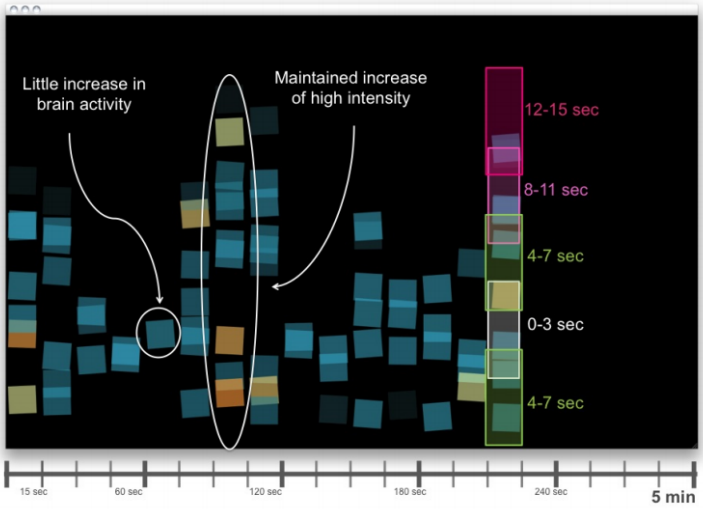

(b)

Figure 7: (a) In the interface from the first version of the neurofeedback application, the current brain activity is visualized by the square changing colors; blue indicating activity below, gray - equal to, and red - above baseline. (b) The interface of the neurofeedback application from the second iteration is shown with additional illustrations describing how it is constructed: The 5-minute timeline shown in the bottom illustrates how the training session is divided into columns of 15 seconds. Within a column squares would appear first (0-3s) in a window in the lower part of the screen, then (4-7 s) in windows above and below the first window and lastly (8-11 s and 12-15 s) in windows above the first two windows. The windows are shown in the rightmost column which was not shown during the experiments. The encircled column illustrates how the user can easily compare the ability to increase brain activity in different time intervals.

along a horizontal axis. At the end of the 5 minute training recording, the interface would consist of 20 columns of squares, see Figure 7b. Thus the interface not only showed the current amplitudes, but also the previous, allowing the user to easily compare methods for increasing the amplitudes. The squares not only indicated when the amplitudes exceed baseline, but also the degree of increase by a change in color, ranging from dark blue to orange (see Figure 8). The degree of increase was calculated from a running mean creating a smooth color flow. The subjects were instructed to create as many squares as possible and preferably with yellow and orange colors. For the baseline recording a similar interface was used, although with squares appearing randomly in the columns and with random color. The subjects were asked to count the yellow and orange squares.

All subjects of both iterations were asked to keep their eyes open for as long as possible, and avoid muscle movements, jaw movements, and swallowing during all recordings to limit artifacts.

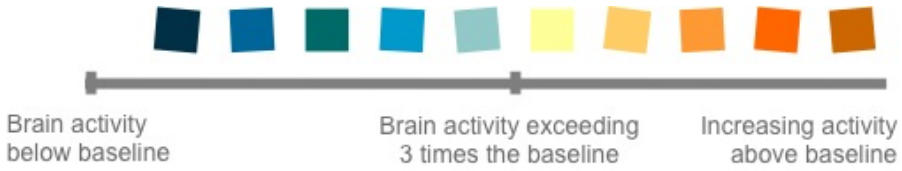

Figure 8: The colors of the squares indicate the intensity of the brain activity.

5. Results and Discussion

In this section we present the results of the experiments, validating the performance of the software, platforms used, and EEG hardware.

5.1. Brain Computer Interface Based on Imagined Finger Tapping

In order to validate the applicability of the platform in decoding imagined left and right finger tapping, the EEG data was bandpass filtered ($8 - 32Hz$) and we used the data in the interval $0.75 - 2.00s$ after stimuli onset as input to the common spatial pattern (CSP) algorithm [28]. One important parameter in the CSP algorithm to be controlled is the number of spatial filters. To determine the number of spatial filters we applied cross-validation and examined the performance (accuracy of classifier) as a function of the training size (number of trials used for training), see Figure 9. The classifier was trained on a balanced set of trials (i.e. equal number of left and right trials), which was carried out 200 times for each training set size.

Figure 9 indicates that we need more than a single spatial filter ($m > 1$). When $m = 2$, for example, two spatial filters are used to maximize the variance for class 1 while minimizing the variance for class 2 and an additional two spatial filters are used to minimize the variance for class 1 while maximizing the

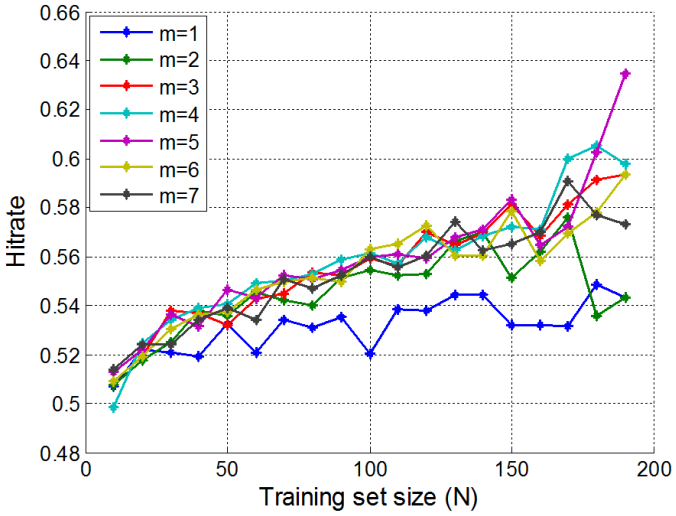

Figure 9: Mean accuracy of left and right imagined finger tapping classification for a single subject. Mean accuracy is based on 200 splits in training and test data. Classification is based on CSP and a quadratic Bayes classifier focusing on bandpass filtered data $8 - 32Hz$ in interval $0.75 - 2.00s$ after onset.

variance for class 2. It is interesting that only a few spatial filters are required to obtain an accuracy close to 60%. We also note that performance is increasing as a function of samples, hence, even better performance can be expected if more samples are collected.

5.1.1. Source Reconstruction and Source Separation

For further validation we applied standard statistical evaluation for significance and correction for multiple comparisons. Thus, we performed a Monte Carlo permutation test [61] to check for significant electrode differences between left and right finger tapping. Figure 10 demonstrates a scalp map of the effect of the averaged response based on left finger tapping minus averaged response based on right finger tapping. The significant channels at given time intervals are highlighted in accordance with the Monte Carlo permutation test conducted using Fieldtrip [62]. Both positive and negative effects are detected as significant with Monte Carlo p-values of 0.012 and 0.001, respectively. A set of 1,000 random permutations were performed. Inspecting Figure 10 reveals significant differences over the left and right hemisphere and more importantly the electrodes contributing to the significant difference between left and right imagined finger tapping are electrodes located close to the premotor area. Thus, it seems that these electrodes are taking over the often reported electrodes C3 and C4 as the main drivers, as C3 and C4 are not present in the Emotiv EEG sensor configuration.

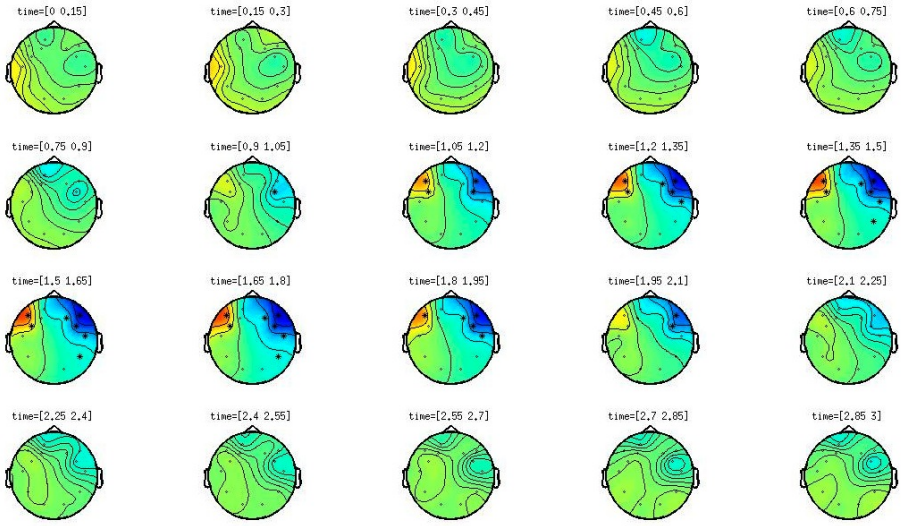

Figure 10: Monte Carlo permutation test for significant difference between averaged left imagined finger tapping response and averaged right imagined tapping. Electrodes located close to the premotor region are detected as significant in the time interval $0.9 - 2.1s$ after stimuli.

To examine the ability to perform reliable 3D EEG imaging based on the data acquired using a Emotiv neuroheadset, source reconstruction was carried out on the bandpass-filtered imagined finger tapping data ($8 - 32Hz$) also used for the classification task and in the non-parametric statistical test. Figure 11 illustrates the mean power of the difference between left and right imagined finger tapping in the interval $0.75 - 2.00s$ post-stimuli. Premotor areas are typically involved in executing the task and in differentiating a left from right imagined movement. This is also the case here to some extent with minor discrimination in the premotor areas and more pronounced discrimination in the more frontally located areas. Note the polarity of the power difference map, with left hemisphere indicating a positive difference and right hemisphere indicating a negative contribution. During the imagined finger tapping part, the contra lateral premotor/motor regions desynchronize (resulting in a decrease in power within the specific frequency range) while the ipsilateral premotor/motor regions first desynchronize shortly and right after synchronize (meaning increased power within the frequency range). The main explanation for the displacement more frontally found in Figure 11, is the uneven distribution of sensors for the Emotiv EPOC system, with most of the sensors positioned frontally. However, large proportions of the occipital and temporal areas are also found to be active by the reconstruction. These apparent visual and temporal source activation differences may, however, be explained by the fact that re-referencing to an average channel is performed prior to source estimation. Since the distribu-

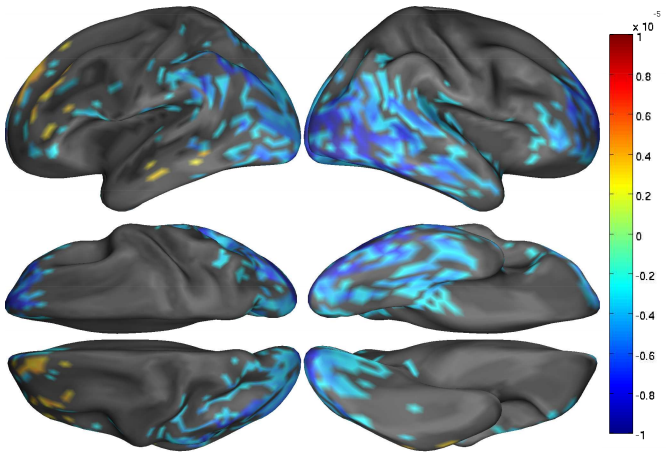

Figure 11: Source reconstruction of mean difference power map between left and right imagined fingertapping.

tion of the sensor locations is highly unevenly distributed, with the majority placed frontally, re-referencing data with a strong frontal activation (e.g. eye blink/movement) to an average reference channel will map part of the frontal activity to the temporal and occipital electrodes. To further test this hypothesis, we investigated the influence of artifacts caused by eye motion on the source reconstruction estimates by removing an eye-related ICA component. Indeed, the removal of the eye movement component seems to improve the source estimates significantly, as demonstrated in Figure 13. The operating regions (frontal areas and slightly pre-motor regions) are more highly visible in this power difference map between the averaged left minus right imagined finger tapping conditions. Similarly, as in Figure 11, the sources are displaced more frontally than typically, and this can be explained by the sensor positioning offered by the Emotiv EPOC system. The source reconstruction was performed offline to ensure a fair comparison with and without removal of the ICA component related to eye movement. The ICA decomposition was performed using the extended informax algorithm supported by EEGLAB.

5.2. Visual Stimulus to Investigate Emotional Responses

Within the Emotiv data, 2×18 ICs have been clustered in 10 out of 10 trials, indicating that these independent components are consistently activated across all trials (Figure 13). Similarly, in the Easycap data, 23 ICs have been clustered within 3 standard deviations of the K-means centroids in 10 out of 10 trials, while 9 ICs have been grouped in 7 out of 10 trials, confirming that temporally independent activations are also grouped across trials in this study (Figure 14). Taking the relative polarity of ICs into account when comparing the two studies, the clustered scalp maps in both experiments suggest left lateralized prefrontal as well as parietal activations in language areas, which integrate motor

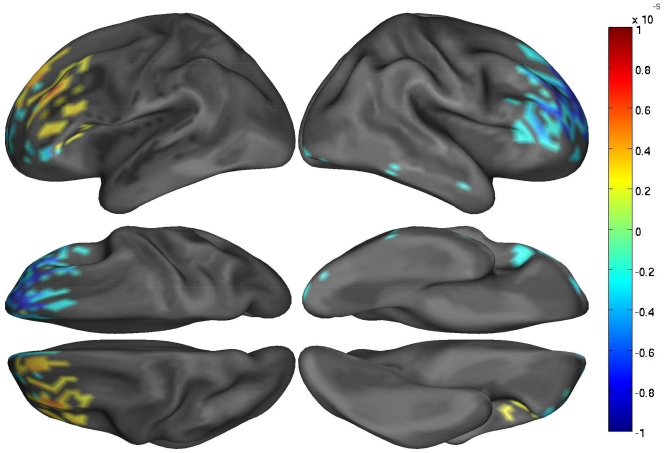

Figure 12: Source reconstruction of mean difference power map between left and right imagined fingertapping. Emotiv EEG data corrected by removal of ICA component associated with eye movement.

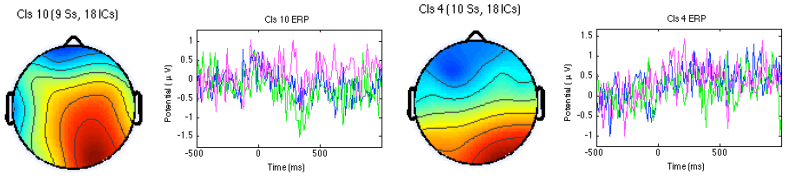

Figure 13: Single-subject EEG neuroimaging study with Emotiv 16 channel neuroheadset: PCA dimensionality reduction and K-means clustering ($K = 10$, $\sigma = 3$) of 140 IC scalp maps, activation time series and event-related changes in power spectra based on 10 trials, each consisting of reading 3×20 emotion (blue), face (green) and hand (pink) related action verbs.

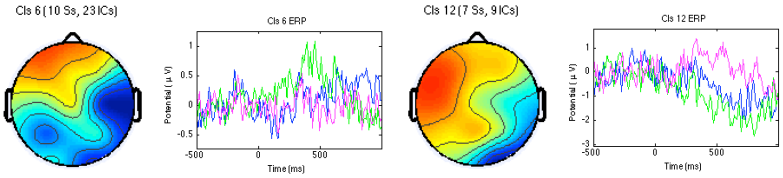

Figure 14: Single-subject EEG neuroimaging study with Easycap 16 channel EEG setup: PCA dimensionality reduction and K-means clustering ($K = 10$, $\sigma = 3$) of 140 IC scalp maps, activation time series and event-related changes in power spectra based on 10 trials, each consisting of reading 3×20 emotion (blue), face (green) and hand (pink) related action verbs.

and semantic aspects connected through the dorsal and ventral streams in the brain [63, 64].

This is in line with results obtained in a recent MRI experiment [46] using the same verbs as in the present EEG study, indicating that premotor neural circuits are activated when passively reading verbs related to face and hand motion and when seeing emotional expressions. Mobile neuroimaging could potentially extend our ability to explore such action-based links between actual motion and emotion in an everyday context, which might in turn reflect imitation of gestures or facial expressions involving mirror neuron circuits in the brain, possibly providing a foundation for higher level feelings of empathy and theory of mind.

5.3. Mobile Interfaces for Neurofeedback

All signal processing of the data for the *Neurofeedback* experiment was done off-line using the EEGLAB [65] plug-in for MATLAB.

Since the alpha frequency band has shown to vary depending on age, possible neurological diseases, and memory performance [51], the upper alpha frequency band had to be determined for each individual. By identifying the peak in the power spectrum, the individual alpha peak (IAF), the upper alpha frequency band was set as a band of 2 Hz above IAF (from IAF to IAF+2Hz). Thus the individuals' upper alpha frequency band were determined from the first baseline recording of every session, and the mean amplitude was calculated for all baseline and training recordings. Two subjects (1 male and 1 female) from the first iteration of the experiment did not complete all training sessions, and were therefore excluded from further analysis.

In addition, it has repeatedly been reported that some subjects, usually called non-responders, are unable to change amplitudes of the brain frequencies significantly [66, 57, 67, 49]. Subjects who did not show a significant increase in the upper alpha frequencies when comparing the very first baseline (baseline 1 in session 1) with the training recordings from Friday (session 5) were considered non-responders. As a result, 3 subjects (2 female, 1 male) from the first iteration and another 3 subjects (2 male, 1 female) from the second iteration were considered non-responders. This left 7 subjects in the first iteration (5 male, 2 female) and 10 subjects in the second iteration (5 male, 5 female) remain for statistical analysis.

The individuals' EEG results from the baseline- and training recordings were normalized in respect to the first baseline Monday (session 1), thereby showing the ability to increase upper alpha (UA) amplitudes in relation to the first baseline in percentage. The results obtained over the week (Monday to Friday) have been plotted in Figure 15. Each line represents a subject's ability to increase UA amplitudes: The red lines represent subjects from the first iteration, the black lines represent subjects from the second iteration and the bold lines represent the non-responders. From the graph it is clear some subjects are more capable of increasing their UA amplitudes and increase above 400%, whereas others experience a decrease (usually the non-responders). In addition, the subjects who get the highest increase are mainly those who use the second iteration interface. However, the variance in the subject ability to increase their UA is also greater. These results suggest the ability to control neural activity is

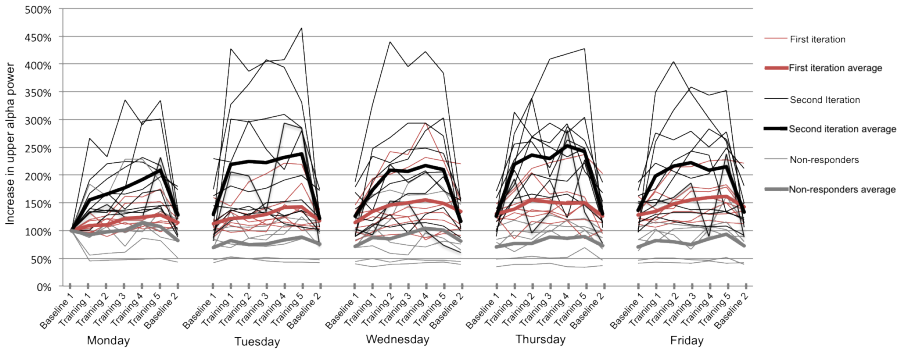

Figure 15: The individuals' upper alpha (UA) amplitude in percentage of the UA amplitude from the fist baseline recording on the first day (Monday). Subjects from first and second iteration as well as the non-responders from both iterations are plotted in red, black and gray, respectively. The average of these groups is marked by bold lines in corresponding colors. All baseline- and training recordings have been plotted in sequence across the week, e.g. Monday will show results from the first baseline, then the 5 training recording, ending with the second baseline, giving a total of 7 points of each day. The results illustrate a large variance in the individual subjects ability to increase UA amplitudes, where subjects from the second iteration were capable of reaching a greater increase, although some subjects were unable to achieve any increase at all (referred to as non-responders).

very individual and that the interface should be supportive of the individual's strategies.

Following the approach of Zoefel et al. [49], we fitted regression lines to the individual UA amplitudes as a function of session number (1-35) and used a one-sample, one-sided t-test to test whether they were significantly greater than zero, which they were in both iterations ($p < 0.05$ and $p < 0.03$ for the first and second iteration respectively). We also compared the regression lines between the iterations using a two-sample, two-sided t-test and found no significant difference ($p > 0.70$). This result, in itself, could indicate that the two types of feedback are equally effective.

This approach does not, however, separate the effect of training (a lasting increase in UA amplitude) from the feedback effect (an immediate increase in UA amplitude during feedback). To isolate the training effect, we again follow the approach of Zoefel et al. who quantified the training effect as the difference between UA amplitude during the first baseline recording in the first session and the first baseline recording in the last session and tested for an increase with a one-sample one-sided t-test. Using this approach we found a significant effect in the first iteration ($p < 0.002$) but not in the second iteration ($p > 0.14$). This result indicates that the interface used in the first iteration was more effective for neurofeedback training.

In addition to this, we are also interested in isolating the feedback effect, which we quantify as the difference between the mean UA amplitude across feedback recordings and the mean UA amplitude across the first and last baseline recording for each session. We compare the feedback effect from the two iterations using a repeated-measures ANOVA with session number as within subject factor and iteration as between groups factor. We found a significant effect of iteration ($F(1, 15) = 11.85$, $p < 0.005$) but no significant effect of session number or the interaction between session and iteration. Based on the lack of effect of the session number, we averaged the feedback effect across session number and subjects within an iteration and found that the mean feedback effect was 0.17 for the first iteration and 0.67 for the second iteration. This result indicates that the interface used in the second iteration was more effective for inducing an immediate increase in UA amplitude.

That the feedback effect was higher in the second group without a corresponding increase in the training effect suggests that the magnitude of UA amplitude during feedback does not completely determine the training effect. This could be due to a ceiling effect, so that UA amplitude during training has no effect above a certain level. Alternatively, it could also mean that the two groups used different strategies for increasing UA amplitude during training and that although the second group's strategy was more efficient for increasing UA amplitude during feedback, it did not increase the training effect. Such strategic differences could be facilitated by the difference in the visual feedback stimulus. In the first group participants needed to constantly look at the feedback stimulus to get feedback, whereas the second group could look elsewhere intermittently and return their gaze to the feedback stimulus only when they wished to learn about their performance. This could change the UA amplitude during feedback without increasing the training effect as could the mere physical differences in the feedback signals.

In summary, our neurofeedback study confirms the findings of Zoefel et al. [49], provides new insights into the effects of the type of feedback provided, and confirms that neurofeedback training is possible with a mobile setup based on the *Smartphone Brain Scanner*.

6. Further perspectives

6.1. Hardware

Current consumer-grade and research-oriented mobile EEG systems are only the first iteration of the hardware. We predict two major directions of the development.

On one hand, the high-density systems will become mobile, pushing for the best possible quality of the acquired signal in naturalistic conditions. The development of these systems will not be primarily focused on making them unobtrusive, fashionable, or consumer-operated. From the spectrum of the features offered by the new EEG hardware, these systems will focus on mobility, portability, and low-cost. They will be used in the more or less classical experiments, controlled and initiated by the researchers.

On the other hand, more consumer-oriented devices will emerge. They will be fitted for particular use-cases, which will allow to make them smaller, concealed, and user-friendly. Such *sensors* will not necessarily be seen as EEG devices, but rather as cognitive state monitoring devices, and in addition to the EEG signal, they may include other electro-physiological signals, such as EMG, ECG, skin conductance etc. Still, the data available from a large number of such systems bought and worn by the consumers for their particular function, may offer an unparalleled opportunity for understanding human brain and cognitive states. Gaining privacy-preserving access to, and analyzing noisy, not-at-all or poorly annotated data originating from brain state, from hundreds or thousands of subjects and collected over days, weeks, or months can become one of the grand challenges for cognitive neuroscience in the next few years.

The development of neuroheadsets and sensors accompanies the development of mobile devices, smartphones and tablets, allowing for personal hubs for interconnected, wearable devices. The increasing processing power and low-energy protocols (e.g., Bluetooth 4.0, NFC) turn our personal space into a busy network of devices (phones, Bluetooth headsets, smart watches, glasses, hearing aids etc.). EEG sensors, even if equipped with a single electrode, can fit naturally in such systems, as long as they can provide certain well-defined value for the user.

6.2. Software

The evolution of the software will be closely coupled with the use-cases of the hardware solutions. For the research-focused high-density mobile hardware, the minimal requirement of data collection and possibly transmission on mobile devices can be easily satisfied with simple software. In such cases, the already existing frameworks, such as EEGLab, can utilize significant processing power of desktop or even server systems, and can even be used for data processing and transmitting the extracted features back to the user.

For more consumer-oriented sensors, real-time applications, possibly operating directly on mobile devices without server connection, need to be developed. The *Smartphone Brain Scanner* is the first framework that enables such development; pushing the limits of what can be done in terms of creating user value by enabling novel EEG applications. As the mobile devices performing the processing grow more powerful, more complex algorithms can be enabled to compensate for noise and low density of the systems.

6.3. Experiments

The vast majority of studies of neural and cognitive functions have so far been set in the laboratory, where the subject is severely restrained in movement, isolated from the surrounding world, and is required to carry out the same limited task repeatedly. This is an impoverished environment we normally live in and are optimized to function in; it totally ignores human agency.

Taking EEG out of the laboratory and into the natural world will allow us to move beyond these constraints. Measuring the EEG of a freely moving

subject will allow us to characterize the neural activity of many important functions. With wearable EEG we can study natural motion such as walking and complex composite motion. We can also study the many cognitive tasks that we constantly perform in their full complexity. Examples include preference-based choice as we select given consumer goods over others, the constant updating of working memory throughout our daily work, and the use of speech in natural social interactions. Measuring the EEG of subjects in rich natural environments will allow us to characterize the neural function of the perceptual systems when they are met with rich multimodal stimuli in which attention is constantly needed to select the relevant stimuli and filter out irrelevant stimuli.

The complexity and variability of data collected in the natural environment will be tremendous compared to the data collected in the laboratory. In order to derive anything meaningful from it, the amount of necessary data will be equally tremendous. Wearable EEG offers an immediate solution as hours, days, even weeks of data can be collected outside of the laboratory; something which is completely unrealistic in lab-based experimentation.

7. Conclusions

Mobile brain imaging, here realized as an EEG system, offers huge promise for many research areas. Here we show our initial work with the *Smartphone Brain Scanner* framework, which can record, analyze, and 3D real-time visualize EEG signals directly on a mobile device, using low-cost, consumer-grade neuroheadsets. The signal obtained in the studies, although of low dimensionality (14 channels) and noisy, can still be successfully used for multiple classical neuroscience applications, including Brain-Computer Interfaces (BCI), analysis of high-level brain activity, and neurofeedback. The features of the presented system make it possible to use in domains such as cognitive psychology, medical applications, social science research, as well as for "self monitoring" as promoted by the Quantified Self community [8].

As the presented framework runs on mobile devices, including tablets and smartphones, it can be coupled with other embedded sensors in a natural way. In this sense, EEG serves as an extension of the sensing capabilities of the already existing devices, and can be used in an integrated way with the other collected data (e.g. location, social interactions, activity level).

We argue that the presented framework enables a wide variety of experiments, and the initial set of these presented in this paper serves as a validation and showcase of the versatility of the framework and general approach. It is now clear that we are at the stage where hardware is powerful and inexpensive enough to be used for mobile brain imaging, while at the same time available algorithms can handle noisy data, allowing us to recover significant information.

The approach to user-oriented and mobile EEG does not end with the notion of researchers using the mobile devices and consumer-grade neuroheadsets to

[8] http://quantifiedself.com/

collect the data from the subjects. We can easily imagine the systems will eventually be able to deliver interesting data to the public, giving them incentive to invest in their own hardware. In this shift, the data would be collected and uploaded by the participants themselves, distributing the cost and difficulty of running experiments. This presents yet more challenges, such as data quality control and privacy. On the other hand, it does give a promise of extremely large datasets created for large populations and over long periods of time, for only little costs.

Acknowledgment

This work is supported in part by the Danish Lundbeck Foundation through CIMBI - Center for Integrated Molecular Brain Imaging (LKH,CS) and a post-doc grant for CS, and by the H. C. Ørsted Foundation. We thank the reviewers for many useful comments and suggestions.

References

[1] C. M. Niel, M. P. Stryker, Modulation of visual responses by behavioral state in mouse visual cortex, Neuron 65 (2010) 472–479.

[2] G. d. Pellegrino, L. Fadiga, L. Fogassi, V. Gallese, G. Rizzolati, Understanding motor events: a neurophysiological study, Experimental Brain Research 91 (1992) 176–180.

[3] V. Gallese, L. Fadiga, L. Fogassi, G. Rizzolati, Action recognition in the premotor cortex, Brain 119 (1996) 593–609.

[4] G. Rizzolati, C. Sinigaglia, The functional role of the parieto-frontal mirror circuit: interpretations and misinterpretations, Nature 11 (2010) 264–274.

[5] U. Hasson, Y. Nir, I. Levy, G. Fuhrmann, R. Malach, Intersubject synchronization of cortical activity during natural vision, science 303 (2004) 1634–1640.

[6] A. Bartels, S. Zeki, Functional brain mapping during free viewing of natural scenes, Human brain mapping 21 (2004) 75–85.

[7] J. P. Dmochowski, P. Sajda, J. Dias, L. C. Parra, Correlated components of ongoing eeg point to emotionally laden attention–a possible marker of engagement?, Frontiers in human neuroscience 6 (2012).

[8] S. Makeig, K. Gramann, T. Jung, T. Sejnowski, H. Poizner, Linking brain, mind and behavior, International Journal of Psychophysiology 73 (2009) 95–100.

[9] Mobi lab matlab plugin, `http://sccn.ucsd.edu/wiki/MoBI_Lab`, 2009. Accessed: 2013-02-27.

[10] K. Gramann, J. Gwin, D. Ferris, K. Oie, T. Jung, C. Lin, L. Liao, S. Makeig, Cognition in action: imaging brain/body dynamics in mobile humans, Reviews in the Neurosciences 22 (2011) 593–608.

[11] S. Slobounov, M. Hallett, C. Cao, K. Newell, Modulation of cortical activity as a result of of voluntary postural sway direction: an eeg study, Neuroscience Letters 442 (2008) doi:10.1016/j.neulet.2008.07.021.

[12] J. A. Caldwell, B. Przinko, J. L. Caldwell, Body posture affects electroencephalographic activity and psychomotor vigilance task performance in sleep-deprived subjects, Clinical Neurophysiology 114 (2003) 23–31.

[13] J. T. Gwin, K. Gramann, S. Makeig, D. P. Ferris, Electrocortical activity is coupled to gait cycle phase during treadmill walking, NeuroImage 54 (2011).

[14] K. Gramann, J. T. Gwin, N. Bigdely-Shamlo, D. P. Ferris, S. Makeig, Visual evoked responses during standing and walking, Frontiers in Human Neuroscience doi: 10.3389/fnhum.2010.00202 (2010).

[15] S. Debener, F. Minow, R. Emkes, K. Gandras, M. Vos, How about taking a low-cost, small, and wireless eeg for a walk?, Psychophysiology (2012).

[16] A. Stopczynski, J. E. Larsen, C. Stahlhut, M. K. Petersen, L. K. Hansen, A smartphone interface for a wireless eeg headset with real-time 3d reconstruction, in: Affective Computing and Intelligent Interaction, Springer, 2011, pp. 317–318.

[17] A. Stopczynski, C. Stahlhut, J. E. Larsen, M. K. Petersen, L. K. Hansen, The smartphone brain scanner: a mobile real-time neuroimaging system, arXiv http://arxiv.org/abs/1304.0357 (2013).

[18] G. Ruffini, S. Dunne, L. Fuentermilla, C. Grau, E. Farrés, J. Marco-Pallarés, P. J. P. Watts, S. R. P. Silva, First human trials of a dry electrophysiology sensor using a carbon nanotube array interface, Sensors and actuators A: Physical 144 (2008) 275–279.

[19] C.-T. Lin, L.-d. Liao, Y.-H. Liu, I.-J. Wang, B.-S. Lin, J.-Y. Chang, Novel dry polymer foam electrodes for long-term eeg measurement, IEEE Transactions on biomedical engineering 58 (2011) 1200–1207.

[20] Y. Chi, Y.-T. Wang, Y. Wang, C. Maier, T.-P. Jung, G. Cauwenberghs, Dry and noncontact eeg sensors for mobile brain-computer interfaces, Neural Systems and Rehabilitation Engineering, IEEE Transactions on 20 (2012) 228–235.

[21] Y. M. Chi, C. Maier, G. Cauwenberghs, Integrated ultra-high impedance front-end for noncontact biopotential sensing, in: Biomedical Circuits and Systems Conference, 2011. BioCAS 2011, Xplore, IEEE, 2011.

[22] D. Looney, P. Kidmose, C. Park, M. Ungstrup, M. L. Rank, K. Rosenkranz, D. P. Mandic, The in-the-ear recording concept: User-centered and wearable brain monitoring, Pulse, IEEE 3 (2012) 32–42.

[23] Y. Yasui, A brainwave signal measurement and data processing technique for daily life applications, Journal of physiological anthropology 28 (2009) 145–150.

[24] L.-d. Liao, C.-Y. Chen, I.-J. Wang, S.-F. Chen, S.-Y. Li, B.-W. Chen, J.-Y. Chang, C.-T. Lin, Gaming control using a wearable and wireless eeg based brain computer interface device with novel dry foam based sensors, Journal of neuroengineering and rehabilitation 9 (2012) http://www.jneuroengrehab.com/content/9/1/5.

[25] A. Stopczynski, C. Stahlhut, J. E. Larsen, M. K. Petersen, L. K. Hansen, The smartphone brain scanner: A mobile real-time neuroimaging system, arXiv preprint arXiv:1304.0357 (2013).

[26] M. Hämäläinen, R. Ilmoniemi, Interpreting magnetic fields of the brain: minimum norm estimates, Med. Biol. Eng. Comput. 32 (1994) 35–42.

[27] R. D. Pascual-Marqui, C. M. Michel, D. Lehmann, Low resolution electromagnetic tomography: a new method for localizing electrical activity in the brain, Int J. Psychophysiol. 18 (1994) 49–65.

[28] J. Müller-Gerking, G. Pfurtscheller, H. Flyvbjerg, Designing optimal spatial filters for single-trial EEG classification in a movement task, Clinical Neurophysiology 110 (1999) 787–798.

[29] F. Babiloni, F. Cincotti, L. Lazzarini, J. Millan, J. Mourino, M. Varsta, J. Heikkonen, L. Bianchi, M. Marciani, Linear classification of low-resolution eeg patterns produced by imagined hand movements, Rehabilitation Engineering, IEEE Transactions on 8 (2000) 186–188.

[30] G. Dornhege, B. Blankertz, G. Curio, K. Müller, Boosting bit rates in non-invasive EEG single-trial classifications by feature combination and multi-class paradigms, IEEE Trans. Biomed. Eng. 51(6) (2004) 993–1002.

[31] B. Blankertz, G. Dornhege, M. Krauledat, K. Muller, V. Kunzmann, F. Losch, G. Curio, The berlin brain-computer interface: Eeg-based communication without subject training, Neural Systems and Rehabilitation Engineering, IEEE Transactions on 14 (2006) 147–152.

[32] M. Ahn, J. H. Hong, S. C. Jun, Feasibility of approaches combining sensor and source features in brain-computer interface, Journal of Neuroscience Methods 204 (2012) 168–178.

[33] M. Besserve, J. Martinerie, L. Garnero, Improving quantification of functional networks with eeg inverse problem: Evidence from a decoding point of view, NeuroImage 55 (2011) 1536–1547.

[34] S. Baillet, J. Mosher, R. Leahy, Electromagnetic brain mapping, IEEE Signal Processing Magazine 18 (2001) 14–30.

[35] C. M. Bishop, Pattern Recognition and Machine Learning, Springer, NY 10013 (USA), 2006.

[36] P. Comon, Independent component analysis, a new concept?, Signal processing 36 (1994) 287–314.

[37] S. Makeig, A. J. Bell, T.-P. Jung, T. J. Sejnowski, Independent component analysis of electroencephalographic data, Advances in Neural Information Processing Systems 8 (1996) 145–151.

[38] A. Delorme, S. Makeig, T. J. Sejnowski, Automatic artifact rejection for eeg data using high-order statistics and independent component analysis, in: International Workshop on ICA.

[39] A. Delorme, T. J. Sejnowski, S. Makeig, Enhanced detection of artifacts from eeg data using higher-order statistics and independant component analysis, NeuroImage 34 (2007).

[40] S. Hoffmann, M. Falkenstein, The correction of eye blink artefacts in the eeg: a comparison of two prominent methods, PLoS ONE 3 (2008) doi:10.1371/journal.pone.0003004.

[41] J. T. Gwin, K. Gramann, S. Makeig, D. P. Ferris, Removal of movement artifact from high-density eeg recorded during walking and running, Journal of Neurophysiology doi: 10.1152/jn.00105.2010 (2010).

[42] S. Makeig, S. Debener, J. Onton, A. Delorme, Mining event-related brain dynamics, Trends in Cognitive Sciences 8 (2004) 204–210.

[43] A. Delorme, J. Palmer, J. Onton, R. Oostenveld, S. Makeig, Independent eeg sources are dipolar, PLoS ONE 7 (2012) doi:10.1371/ journal.pone.0030135.

[44] A. Delorme, T. Mullen, C. Kothe, Z. Acar, N. Bigdely-Shamlo, A. Vankov, S. Makeig, Eeglab, sift, nft, bcilab, and erica: new tools for advanced eeg processing, Computational intelligence and neuroscience 2011 (2011) 10.

[45] F. Pulvermüller, L. Fadiga, Active perception: sensorimotor circuits as a cortical basis for language, Nature Neuroscience 11 (2010) 351–360.

[46] R. Moseley, F. Carota, O. Hauk, B. Mohr, F. Pulvermüller, A role for the motor system in binding abstract emotional meaning, Cerebral Cortex doi:10.1093/cercor/bhr238 (2011) 1–14.

[47] I. T. Jolliffe, Principal Component Analysis, Springer Series in Statistics, Springer, 1986 (2002).

[48] S. Hanslmayr, P. Sauseng, M. Doppelmayr, M. Schaubus, W. Klimesch, Increasing individual upper alpha power by neurofeedback improves cognitive performance in human subjects, Applied psychophysiology and biofeedback 30 (2005) DOI: 10.1007/s10484–005–2169–8.

[49] B. Zoefel, R. J. Huster, C. S. Herrmann, Neurofeedback training of the upper alpha frequency band in EEG improves cognitive performance., NeuroImage 54 (2011) 1427–31.

[50] J. J. Foxe, A. C. Snyder, The role of alpha-band brain oscillations as a sensory suppression mechanism during selective attention, Frontiers in Psychology 2 (2011) 1–13.

[51] W. Klimesch, EEG alpha and theta oscillations reflect cognitive and memory performance: a review and analysis., Brain research. Brain research reviews 29 (1999) 169–95.

[52] J. Tidwell, Designing Interfaces - patterns for effective interaction design, O' Reilly, 2011.

[53] T. Egner, T. F. Zech, J. H. Gruzelier, The effects of neurofeedback training on the spectral topography of the electroencephalogram, Clinical Neurophysiology 115 (2004) 2452–2460.

[54] T. Hinterberger, N. Neumann, M. Pharn, A. Kübler, A. Grether, N. Hofmayer, B. Wilhelm, H. Flor, N. Birbaumer, A multimodal brain-based feedback and communication system, Experimental Brain Research 154 (2004) 521–526.

[55] N. Neumann, A. Kübler, J. Kaiser, T. Hinterberger, N. Birbaumer, Conscious perception of brain states: mental strategies for brain-computer communication, Neuropsychologia 41 (2003) 1028–1036.

[56] D. Vernon, T. Egner, N. Cooper, T. Compton, C. Neilands, A. Sheri, J. H. Gruzelier, The effect of training distinct neurofeedback protocols on aspects of cognitive performance, International Journal of Psychophysiology 47 (2003) 75–85.

[57] H. Gevensleben, B. Holl, B. Albrecht, C. Vogel, D. Schlamp, O. Kratz, P. Studer, A. Rothenberger, G. H. Moll, H. Heinrich, Is neurofeedback an efficacious treatment for ADHD? A randomised controlled clinical trial., Journal of child psychology and psychiatry, and allied disciplines 50 (2009) 780–9.

[58] H. Heinrich, H. Gevensleben, U. Strehl, Annotation: neurofeedback - train your brain to train behaviour, Journal of child psychology and psychiatry, and allied disciplines 48 (2007) 3–16.

[59] C. B. F. Jensen, M. K. Petersen, J. E. Larsen, A. Stopczynski, C. Stahlhut, M. G. Ivanova, T. Andersen, L. K. Hansen, Spatio temporal media components for neurofeedback, in: Proceedings of 2013 IEEE International Conference on Multimedia and Expo (ICME).

[60] C. Jensen, M. Ivanova, Training your brain on a tablet, 34th Annual International ... 54 (2011) 50946026.

[61] E. Maris, R. Oostenveld, Nonparametric statistical testing of eeg-and meg-data, Journal of Neuroscience Methods 164 (2007) 177–190.

[62] R. Oostenveld, P. Fries, E. Maris, J. Schoffelen, Fieldtrip: open source software for advanced analysis of meg, eeg, and invasive electrophysiological data, Computational intelligence and neuroscience 2011 (2011) 1.

[63] T. Rolheiser, E. A. Stamatakis, L. K. Tyler, Dynamic processing in the human language system: Synergy between the arcuate fascicle and extreme capsule, The Journal of Neuroscience 31 (2011) 16949–16957.

[64] H. Axer, C. M. Klingner, A. Prescher, Fiber anatomy of dorsal and ventral language streams, Brain & Language http://dx.doi.org/10.1016/j.bandl.2012.04.015 (2012).

[65] A. Delorme, S. Makeig, Eeglab: an open source toolbox for analysis of single-trial eeg dynamics including independent component analysis, Journal of neuroscience methods 134 (2004) 9–21.

[66] T. Fuchs, N. Birbaumer, W. Lutzenberger, J. H. Gruzelier, J. Kaiser, Neurofeedback treatment for attention-deficit/hyperactivity disorder in children: a comparison with methylphenidate., Applied psychophysiology and biofeedback 28 (2003) 1–12.

[67] J. F. Lubar, M. O. Swartwood, J. N. Swartwood, P. H. O'Donnell, Evaluation of the effectiveness of EEG neurofeedback training for ADHD in a clinical setting as measured by changes in T.O.V.A. scores, behavioral ratings, and WISC-R performance., Biofeedback and self-regulation 20 (1995) 83–99.